Ngok et al., http://www.jcb.org/cgi/content/full/jcb.201207009/DC1

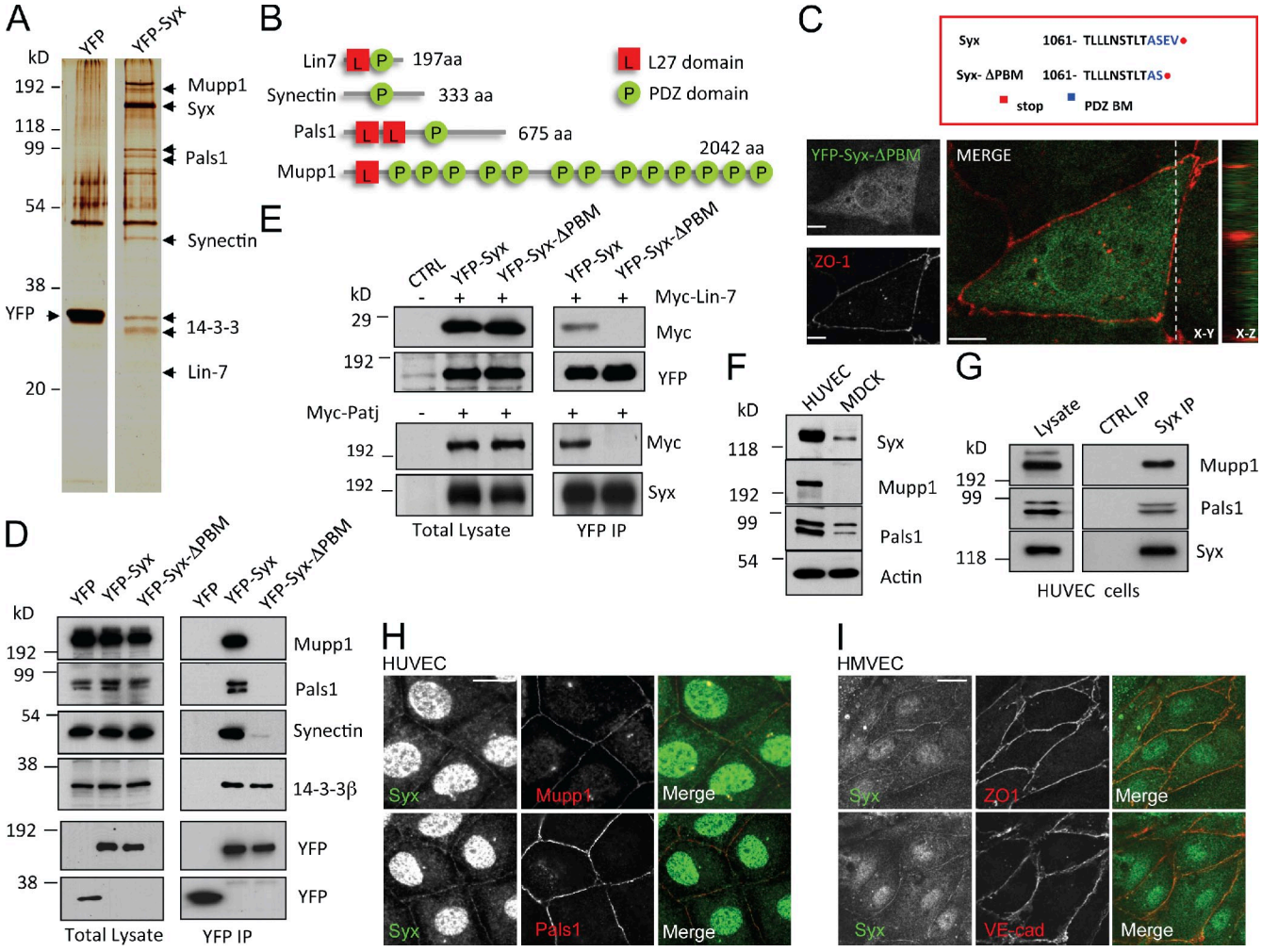

Figure S1. **Syx interacts with either the CRB complex or synectin via its C-terminal PBM.** (A) Proteins coimmunoprecipitated with YFP-Syx in HeLa cells and identified by mass spectrometry (Table S1). (B) Schematic of domain structure of Syx-interacting proteins shows the common presence of PDZ domains. (C) A YFP-Syx mutant devoid of the PDZ-binding motif (PBM) is not targeted to the cell junctions when expressed in MDCK cells. The dotted line corresponds to the x-z cross section. (D) Immunoprecipitation of YFP, YFP-Syx, and YFP-Syx-ΔPBM in HeLa cells. Disruption of the Syx PDZ-binding motif (Syx.ΔPBM) caused loss of binding to Mupp1, Patj, Pals1, and synectin but not of 14-3-3. (E) Myc-fused Lin7 and PATJ coimmunoprecipitate with YFP-Syx but not with YFP-Syx-ΔPBM in HeLa cells. (F) Endogenous expression of the indicated proteins in HUVECs and MDCK cells. (G) Immunoprecipitation of endogenous Syx from HUVECs brings down Mupp1 and Pals1. (H) Endogenous Syx colocalizes with Mupp1 and Pals1 in HUVECs. The nuclear staining of the anti-Syx chicken polyclonal antibody is likely an artifact, as it is not removed by *syx* knockdown. (I) Syx localizes at intercellular junctions in HMVECs. Endogenous Syx colocalizes with the cell junction markers ZO1 and VE-cadherin in confluent HMVECs. The nuclear staining is likely an artifact, as it is not removed by depletion of endogenous Syx (not depicted). CTRL, control; IP, immunoprecipitation. Bars: (C) 10 µm; (H and I) 20 µm.

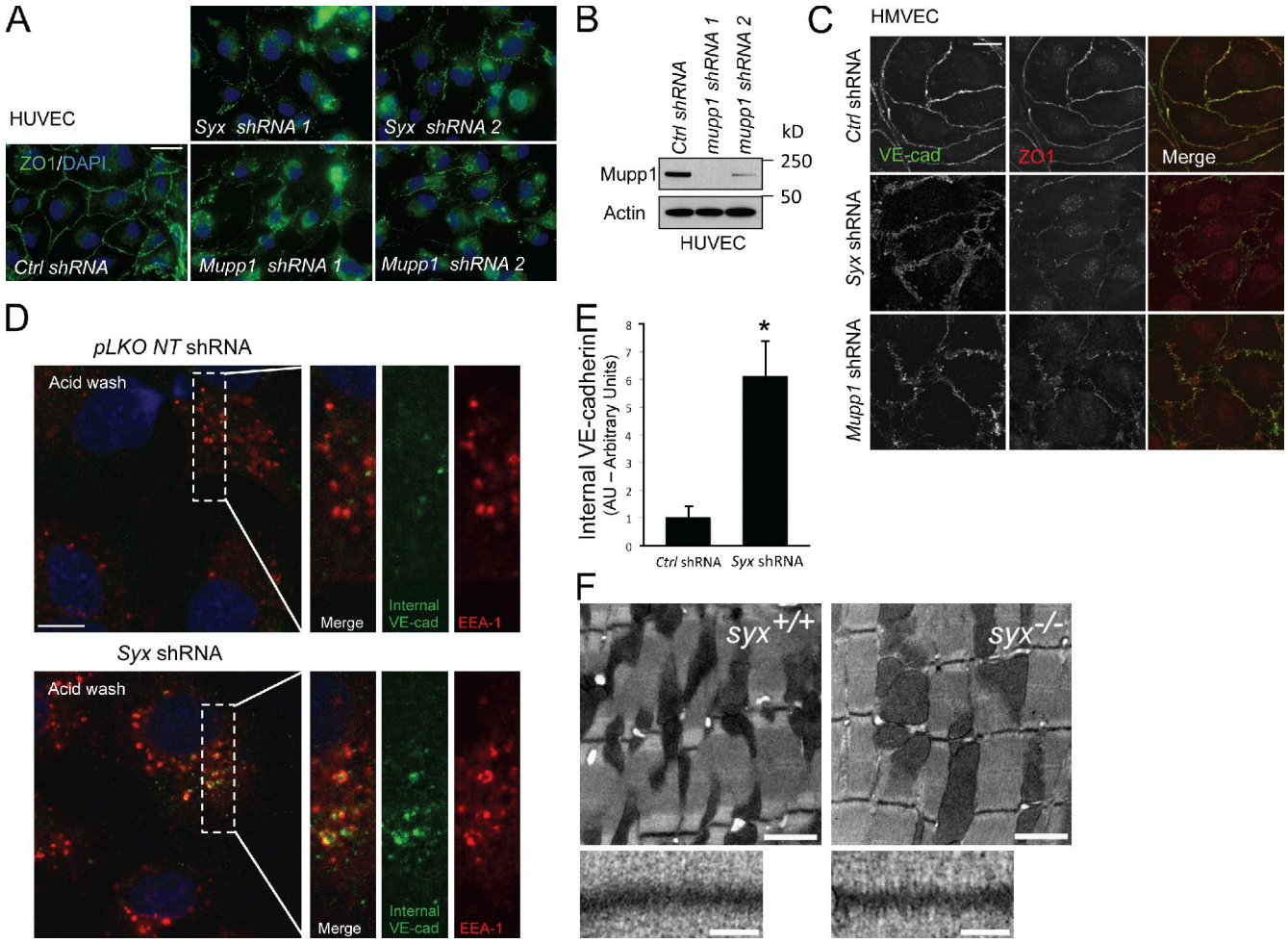

Figure S2. **Mupp1 promotes endothelial junction stability and Syx-depleted cells exhibit increased VE-cadherin endocytosis.** (A) Effect of silencing either Syx or Mupp1 with two nonoverlapping shRNAs, each on the junctional localization of ZO1 in confluent HUVEC monolayers. (B) Silencing efficacy of the *mupp1* shRNA constructs in HUVECs. (C) Effect of silencing endogenous Syx or Mupp1 on the localization of ZO1 and VE-cadherin in HMVECs. (D) Effect of silencing endogenous Syx on the internalization of VE-cadherin (VE-cad), as monitored by the uptake of anti–VE-cadherin antibody (BV6; 37°C for 30 min) and its colocalization with the early endosome marker EEA1 in HUVECs, and subsequent acid wash (see Materials and methods). The dotted box is magnified to the right. pLKO NT denotes control nontarget shRNA. (E) Quantification of internalized VE-cadherin fluorescence intensity using ImageJ (means ± SD, $n = 9$; *, $P < 0.01$). (F) Electron micrographs of sarcomeres in the $syx^{+/+}$ and $syx^{-/-}$ myocardia. The magnified fields under each micrograph show high-resolution images of intercalated disks from each mouse genotype. Ctrl, control. Bars: (A and C) 20 µm; (D) 10 µm; (F, top) 0.5 µm; (F, bottom) 0.05 µm.

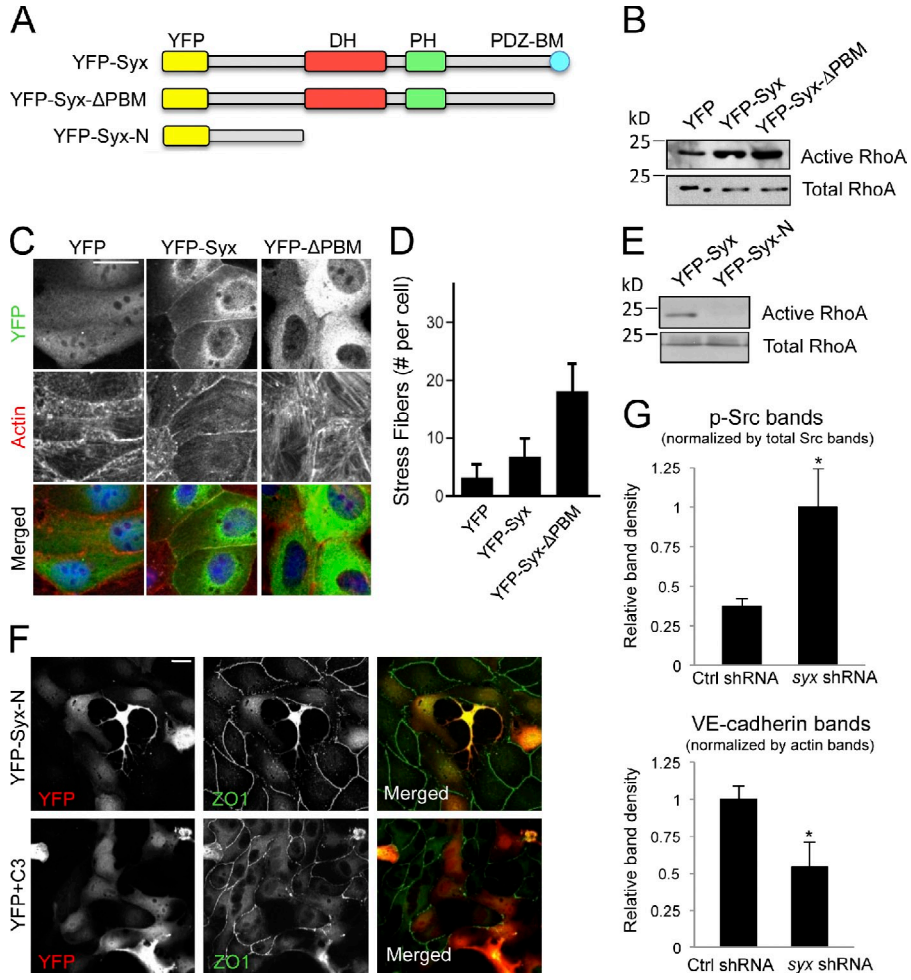

Figure S3. **Syx localization and activity determine junction integrity.** (A) Schemes of the domain structure of YFP-Syx, YFP-Syx-ΔPBM, and YFP-Syx-N. DH, Dbl homology; PH, pleckstrin homology; BM, binding motif. (B) RhoA activity levels in lysates of HeLa cells ectopically expressing the indicated constructs. (C) Effect of expressing YFP, YFP-Syx, or YFP-Syx-ΔPBM on F-actin pattern in MDCK cells (DAPI, blue). (D) Quantification of the mean number of stress fibers per cell transfected with the indicated constructs (means ± SD, $n = 20$). (E) RhoA activity levels in lysates of HeLa cells expressing either YFP-Syx or YFP-Syx-N. (F) Comparison of the effect of expressing YFP-fused Syx N terminus domain (YFP-Syx-N) to the expression of C3 exotransferase (coexpressed with YFP for visualization) on MDCK morphology and junction integrity (using ZO1 as a marker). (G) Densitometric analysis (using ImageJ) of p-Src and total VE-cadherin bands shown in Fig. 3 D (means ± SD, $n = 3$; *, $P < 0.01$). Ctrl, control. Bars, 20 µm.

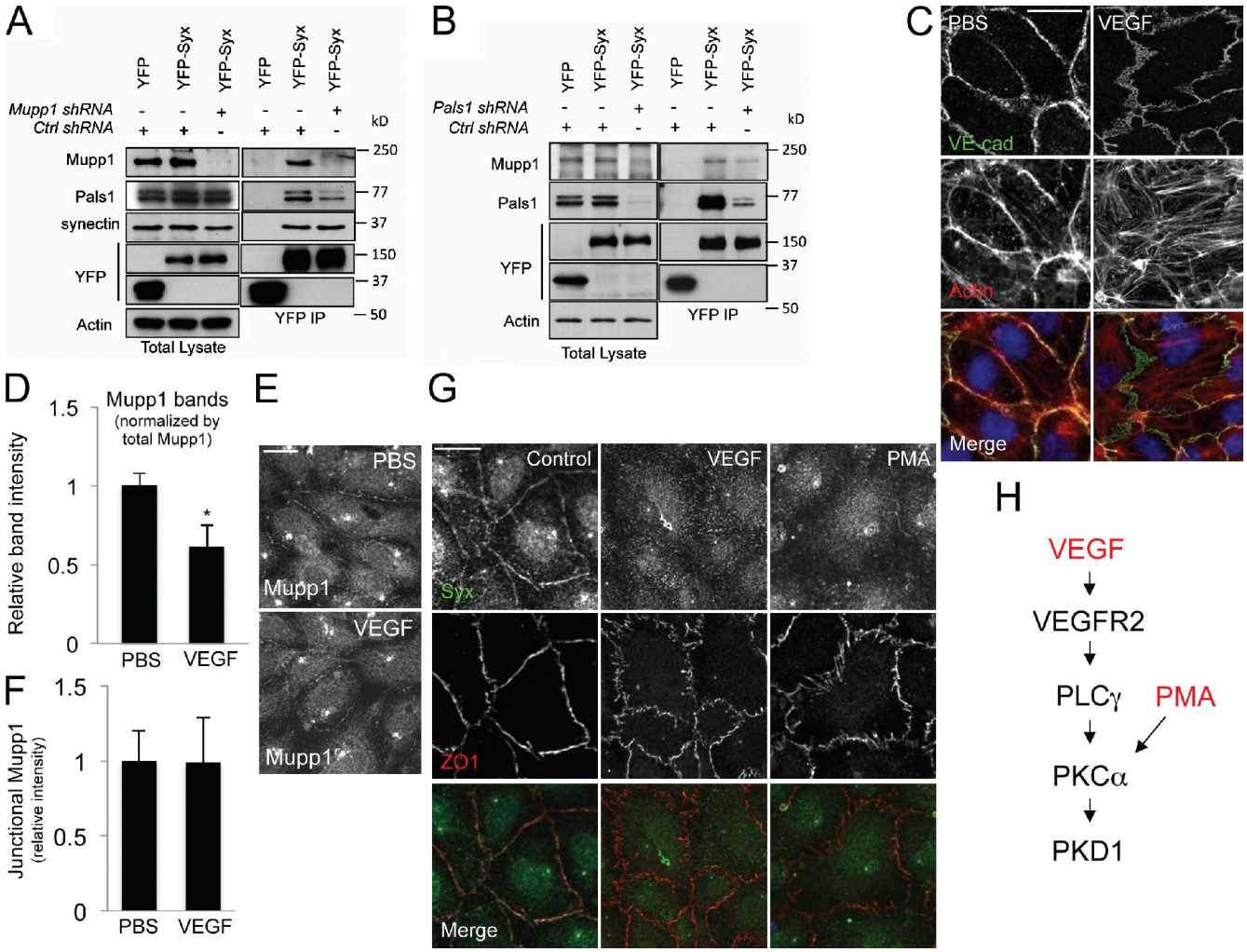

Figure S4. **VEGF and PMA induce Syx translocation away from Mupp1 and the cell junctions.** (A) Immunoprecipitation of YFP or YFP-Syx in nontarget or Mupp1-depleted HeLa cells. Immunoprecipitates were immunoblotted for the indicated binding proteins. (B) As in A, immunoprecipitation was performed in nontarget or Pals1-depleted HeLa cells, and samples were analyzed by Western blot analysis. (C) Effects of 50 ng/ml VEGF (30 min) on VE-cadherin (VE-cad) localization and cortical actin organization in confluent HUVECs. (D) Densitometric analysis (using ImageJ) of Mupp1 bands shown in Fig. 6 A (means ± SD, $n = 3$; *, $P < 0.01$). (E) Effects of 50 ng/ml VEGF (30 min) treatment on the junctional localization of endogenous Mupp1 in HUVEC monolayers. (F) Quantification of junctional Mupp1 fluorescence intensity using ImageJ (mean ± SD, $n = 6$). (G) Effects of 100 nM PMA treatment (15 min) on Syx and ZO1 localization in confluent HUVECs. Note that the PMA-induced loss of junctional Syx is similar to the one induced by VEGF. (H) Scheme of signaling events downstream of VEGF or PMA treatment, leading to PKD1 activation. Ctrl, control; IP, immunoprecipitation. Bars, 20 µm.

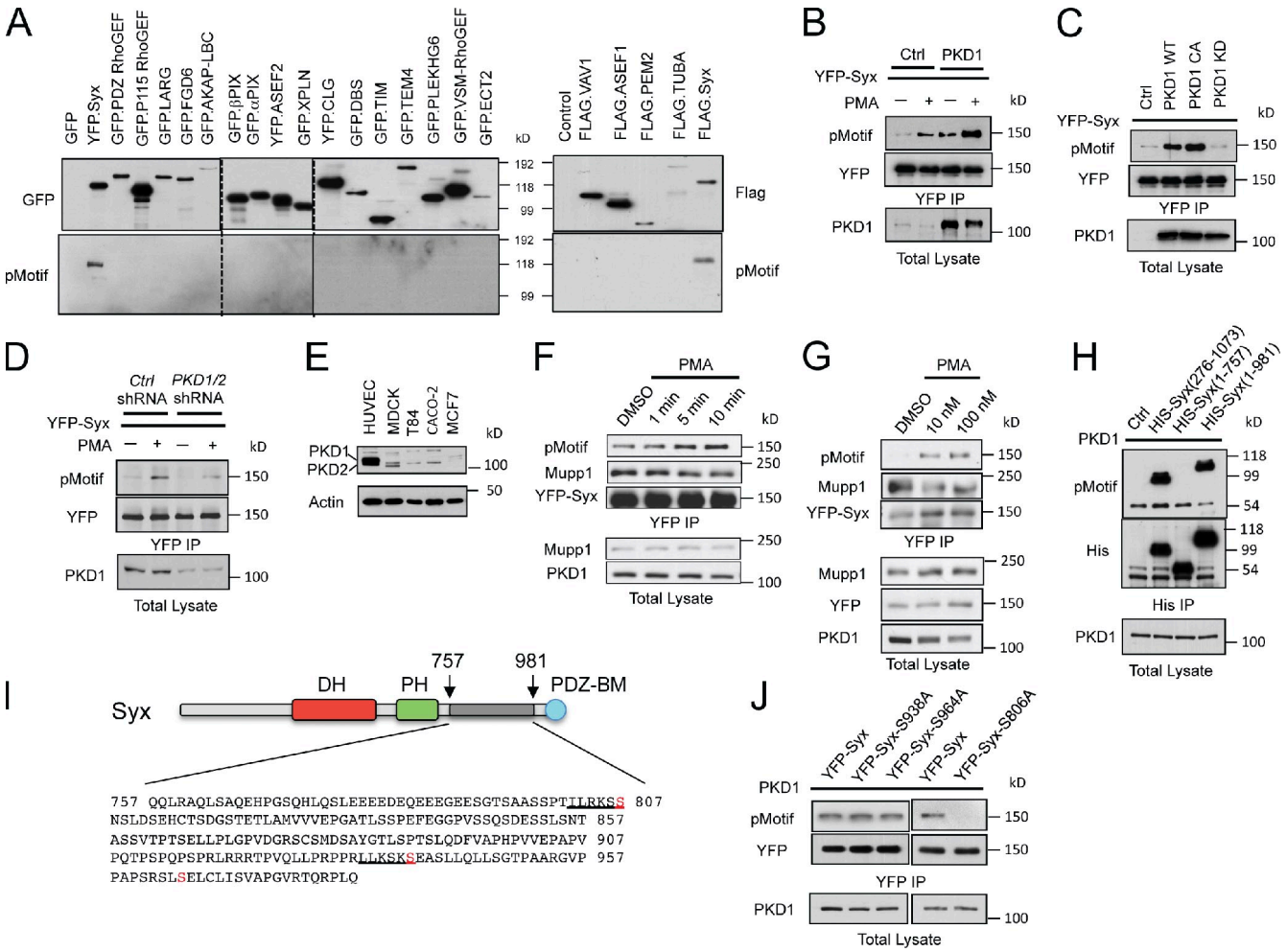

Figure S5. **PKD1 mediates Syx phosphorylation at serine 806.** (A) A series of either GFP/YFP or FLAG-fused GEFs were immunoprecipitated and probed by immunoblotting with an antibody specific to a PKD-phosphorylated consensus motif (pMotif). The anti-GFP antibody recognizes both GFP- and YFP-tagged proteins. (B) Effect of 100 nM PMA treatment (15 min) on the phosphorylation level of YFP-Syx coexpressed with either an empty vector (control [Ctrl]) or wild-type PKD1 in HeLa cells. (C) Effect of ectopically expressing wild-type PKD1, constitutively active (CA) PKD1, or kinase-dead (KD) PKD1, on the phosphorylation level (detected by pMotif) of coexpressed YFP-Syx in HeLa cells. (D) Effect of silencing the major endogenous PKD isoforms 1 and 2 on PMA-induced phosphorylation of YFP-Syx (detected by pMotif) in HeLa cells. VE-cad, VE-cadherin. (E) Immunoblot showing the expression level of endogenous PKD isoforms in HUVECs, MDCK, and in three other epithelial cell types. (F) Time dependence of 100 nM PMA-induced phosphorylation of YFP-Syx expressed in HeLa cells. The extent of Mupp1 coimmunoprecipitated with YFP-Syx decreases with time as PKD-mediated phosphorylation increases. (G) Dose dependence of PMA-induced (15 min) YFP-Syx phosphorylation in a HeLa cell coexpressing wild-type PKD1. The increased PKD-mediated phosphorylation of YFP-Syx correlates with decreased Mupp1 coimmunoprecipitation upon treatment of cells with either 10 or 100 nM PMA. (H) Immunoblot of HeLa cells coexpressing wild-type PKD1 and several truncation mutants of His-tagged Syx, indicating that the PKD-mediated phosphorylation site is between residues 757 and 981 of Syx. (I) Scheme of Syx (Plekhg5) showing the location and the sequence of the region containing the three potential phosphorylation sites identified by mass spectrometry; underlined sites conform to a PKD phosphorylation motif (Döppler et al., 2005), and the phosphorylatable serines are shown in red. (J) Immunoblot of HeLa cells expressing YFP-tagged Syx in which one of three potential phosphorylation sites was mutated from serine to alanine. Only the replacement of S^{806} abolished detection with the pMotif antibody.

Table S1. **Syx-interacting proteins**

Name	Alias	Accession no.	Theoretical size	Peptide count (unique/total)
			kD	
PLEKHG5	Syx1,Tech, and Gef20	NM_020631	111	54/127
MUPP1	Mpdz1	NM_003829	219	30/51
PALS1	Mpp5	NM_022474	77	21/41
GIPC1	Synectin, Tip2, and Nip	NM_202494	36	8/14
14-3-3ε	YWHAE	NM_006761	29	10/47
14-3-3α/β	YWHAB	NM_003404	28	3/11
14-3-3γ	YWHAG	NM_012479	28	5/13
14-3-3ζ/δ	YWHAZ	NM_145690	28	6/16
14-3-3η	YWHAH	NM_003405	28	4/10
14-3-3τ	YWHAQ	NM_006826	28	3/11
LIN-7	Veli3 and Mals3	NM_018362	22	8/18

Accession numbers (obtained from the GenBank), theoretical size (in kilodaltons), and peptide count (unique versus total) of all proteins were identified by mass spectrometry (see Materials and methods) to coimmunoprecipitate with YFP-Syx in HeLa cells.

Reference

Döppler, H., P. Storz, J. Li, M.J. Comb, and A. Toker. 2005. A phosphorylation state-specific antibody recognizes Hsp27, a novel substrate of protein kinase D. *J. Biol. Chem.* 280:15013–15019. http://dx.doi.org/10.1074/jbc.C400575200